

AUTOMATIC DETECTION OF HUMAN PARASITE WORM USING
MICROSCOPIC IMAGE

RUSHDINA BINTI ROSLAN

This thesis is submitted as partial fulfillment of the requirements for the award of the
Bachelor of Electrical Engineering (Electronics)

Faculty of Electrical & Electronics Engineering
Universiti Malaysia Pahang

MAY, 2012

I declare that this thesis entitled "*AUTOMATIC DETECTION OF HUMAN PARASITE WORM USING MICROSCOPIC IMAGE*" is the result of my own research except as cited in the references. The thesis has not been accepted for any degree and is not concurrently submitted in candidature of any other degree.

Signature :

Name : RUSHDINA BINTI ROSLAN

Date : 21st June 2012

“I hereby acknowledge that the scope and quality of this thesis is qualified for the award of the Bachelor Degree of Electrical Engineering.”

Signature :

Name: DR. KAMARUL HAWARI BIN GHAZALI

Date: 21st June 2012

Specially dedicated to
My beloved parents
My brother and two sisters
My lecturers
My teachers
And all friends

ACKNOWLEDGMENT

Alhamdulillah, the highest thanks to God because with His Willingness I can complete the final year project in time.

I would like to express my gratitude to my dedicated supervisor, Dr. Kamarul Hawari bin Ghazali for guiding this project with clarity and that priceless gift of getting things done by sharing his valuable ideas as well as his knowledge.

The great cooperation, kindheartedness and readiness to share worth experiences that have been shown by him will be always appreciated and treasured by me. Once again, thank you very much.

ABSTRACT

This project investigates about the development of automatic detection of egg of human parasites using microscopic images. The MATLAB software is the tool to analyse the image processing technique applied in this research. The stages of image processing technique are image acquisition, processing, classification and testing. The input image is a microscopic image with three different resolutions. The experiment parasites are found in faecal samples provided by doctor at HUSM. This project had been categorized the two types of parasites worm which is Roundworm, *Ascaris Lumbricoides* and Whipworm, *Trichuris Trichiura*. The identification of the parasites is based on its eggs roundness, shape and smoothness characteristics. The MATLAB software recognized the types of parasite based on classification that had been done before. The image processing used are edge detection, filling, morphological operation and others. The image of egg parasite will be expected to appear without other subjects inside result image. This project will give benefit to biomedical industry and human health as it acts as a specialist to acknowledge a patient's condition by the existence of types of parasite living in one's body.

ABSTRAK

Projek ini mengkaji tentang pembangunan pengesanan telur parasit manusia menggunakan imej mikroskop secara automatik. Program MATLAB merupakan alat untuk menganalisis teknik pemprosesan imej yang digunakan dalam kajian ini. Peringkat-peringkat teknik pemprosesan imej ialah pengambilan imej, pemprosesan, penyusunan mengikut kelas dan pengujian. Input imej merupakan sebuah imej mikroskop dengan tiga nilai resolusi yang berbeza. Parasit digunakan dalam eksperimen ditemui di sampel 'faecal' yang disediakan oleh doktor di HUSM. Projek ini mengkategorikan dua jenis cacing parasit iaitu Roundworm, *Ascaris Lumbricoides* dan Whipworm, *Trichuris Trichiura*. Identifikasi parasit adalah berdasarkan sifat bulat, bentuk dan kejelasan. Program MATLAB mengenalpasti jenis parasit berdasarkan klasifikasi yang dibuat sebelumnya. Pemprosesan imej menggunakan pengesanan bucu, pemenuhan, operasi morfologi dan lain-lain. Telur parasit dijangka untuk muncul dengan sebarang subjek lain dalam imej terakhir. Projek ini akan member faedah kepada industri biomedik dan kesihatan manusia kerana ia bertindak sebagai pakar untuk mengetahui keadaan pesakit dengan kewujudan jenis parasit yang terdapat dalam tubuh seseorang.

TABLE OF CONTENTS

CHAPTER	TITLE	PAGE
	TITLE OF PROJECT	i
	DECLARATION	ii
	DECLARATION BY SUPERVISOR	iii
	DEDICATION	iv
	ACKNOWLEDGEMENT	v
	ABSTRACT	vi
	ABSTRAK	vii
	TABLE OF CONTENTS	viii
	LIST OF TABLES	xi
	LIST OF FIGURES	xii
	LISTOF	xiv
	SYMBOLS/ABBREVIATIONS/NOTATIONS/TERMINOLOGY	
	LIST OF APPENDICES	xv

1	INTRODUCTION	
	1.1 Project background	1
	1.2 Project Objective	5
	1.3 Project Scopes	5
	1.4 Problem Statement	6
2	LITERATURE REVIEW	
	2.1 Literature Review	7
3	METHODOLOGY	
	3.1 Introduction	11
	3.2 System Flow	12
	3.2.1 Eggs of Parasite Data Information	13
	3.2.2 Processing Image	15
	3.2.3 Making Decision	21
4	RESULT AND DISCUSSION	
	4.1 Results	
	4.1.1 Roundworm, Ascaris Lumbricoides	22
	4.1.2 Whipworm, Trichuris Trichiura	27
	4.1.3 Size of roundness of detected eggs	30
	4.2 Discussion	33

5	CONCLUSION	
	5.1 Conclusion	34
	5.2 Recommendation	35
6	REFERENCE	36
	APPENDIX	
	APPENDIX A	39
	APPENDIX B	40

LIST OF TABLES

TABLE NO.	TITLE	PAGE
4.1	The size of eggs image with 10 resolutions	31
4.2	The size of eggs image with 20 resolutions	32
4.3	The size of eggs image with 40 resolutions	32

LIST OF FIGURES

FIGURE NO.	TITLE	PAGE
1.1	Infected digestive system	2
1.2	Roundworm, <i>Ascaris Lumbricoides</i>	2
1.3	Whipworm, <i>Trichuris Trichuria</i>	2
1.4	Gastro-intestinal tract in human	2
1.5	Three figures of microscopic images	3
3.1	Processing stage	12
3.2	HUSM at Kubang Kerian	13
3.3	Microscopic input image of a) Roundworm b) Whipworm	14
3.4	The appeared edges image	16
3.5	The dilated image	16
3.6	The filling image	17
3.7	The cleared border image	18
3.8	The eroded image	18
3.9	The result image	20
4.1	Detected Roundworm eggs with 10nm resolutions	23
4.2	Step by step to detect the Roundworm egg with 10nm resolutions	23
4.3	Detected Roundworm eggs with 20nm resolutions	24
4.4	Step by step to detect the Roundworm egg with 20nm resolutions	24
4.5	Detected Roundworm eggs with 40nm resolutions	25
4.6	Step by step to detect the Roundworm egg with 40nm resolutions	26
4.7	Detected Whipworm eggs with 10nm resolutions	27

4.8	Step by step to detect the Whipworm egg with 10nm resolutions	28
4.9	Detected Whipworm eggs with 20nm resolutions	28
4.10	Step by step to detect the Whipworm egg with 20nm resolutions	29
4.11	Detected Whipworm eggs with 40nm resolutions	29
4.12	Step by step to detect the Whipworm egg with 40nm resolutions	30

LIST OF SYMBOLS/ABBREVIATIONS/NOTATIONS/TERMINOLOGY

n	-	nano
m	-	meter
π	-	pi = 3.14159

LIST OF APPENDICES

APPENDIX	TITLE	PAGE
A	GUI Builder	39
B	Input images	40

Chapter 1

INTRODUCTION

1.1 Project Background

– The intestinal parasites are common infections world-wide and cause many illnesses such as irritation, damaged tissue, parasitic contamination, microorganism intrusion, allergic response by the human body itself. The intestinal parasites are parasites that populate the gastro-intestinal tract in humans and other animals. The parasites in the intestines can be classified into two classes. These are Protozoa and Helminthes. The Helminthes are separated many categories such as Fasciola, Schistosoma, Ascaris, Hookworm, Trichuris, Taenia and Enterobius. *Ascaris lumbricoides* is a parasitic nematode (roundworm). *A. lumbricoides* invades the gastrointestinal tract after consumption of its eggs in contaminated food or drink or from fomites. *A. lumbricoides* migrates from the intestines to the lungs via the bloodstream. It is then swallowed and returned to the small intestine, where it reproduces. A high parasite load can cause nutritional deficiencies, especially in those consuming marginal diets.

Trichuris trichiuria, the Whipworm, causes infestation after consumption of egg contaminating foodstuffs. It reproduces in the intestinal tract and the eggs are found in the feces. Heavy parasite loads may result in dysentery in the host.



Figure 1.1: Infected digestive system

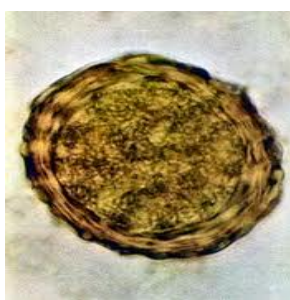


Figure 1.2: Roundworm, *Ascaris Lumbricoides*



Figure 1.3: Whipworm, *Trichuris Trichuria*

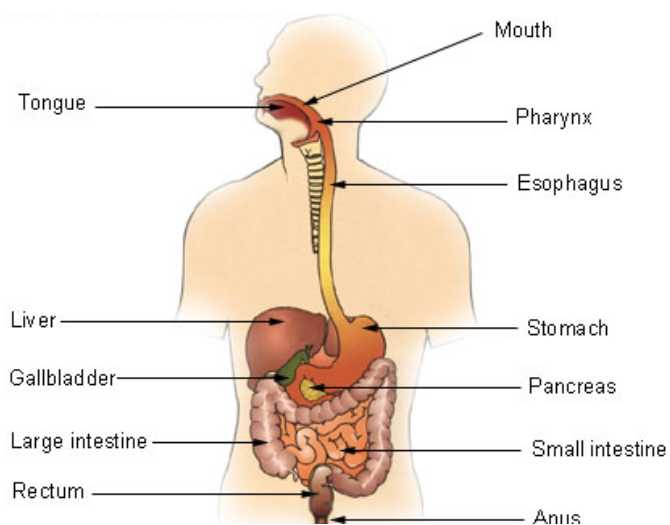


Figure 1.4: Gastro-intestinal tract in human

In general, identification and detection are direct methods primarily developed to define presence or absence, and to discriminate among parasite groups. Diagnostic techniques, on the other hand, can be either direct or indirect in nature and tend to define the disease state of an individual or animal. In some cases identification, detection and diagnosis are mutually exclusive.

Diagnosis is most often made by detection of the eggs in a faecal specimen. However, whole specimens may be obtained from the mouth or nares after the worms have migrated to these sites. Whole specimens have also been obtained surgically from the intestines. The cysts and eggs of endoparasites, which cause infection inside human body may be found in feces which aids in the detection of the parasite in the human host while also providing a means for the parasitic species to exit the current host and enter other hosts. The human body exposed to parasites by food, and water sources, soil, vegetables, fruits, animals and others.

Microscopy plays a prominent role in the identification of microorganisms, and in all likelihood, will continue to do so in the foreseeable future. Microscopic image processing is the digital image processing technique to process, analyze and present images obtained from a microscope. A number of manufacturers of microscope now specifically design in features that allow the microscopes to interface to an image processing system. Image processing for microscopy application begins with fundamental techniques intended to most accurately reproduce the information contained in the microscopic sample. This might include adjusting the brightness and contrast of the image, averaging images to reduce image noise and correcting for illumination non-uniformities.



Figure 1.5: Three figures of microscopic images

The current practice of diagnose parasite rely to human services of medical team such as doctor and physician. To treat human for parasites, the doctor must diagnose the specific parasite. He will perform tests based on human symptoms. The diagnosis will be done step by step by firstly, produce a stool specimen in a clean, dry container. Then, a blood sample is allowed to be taken to check for parasites that can be found in human blood. After that, a blood sample is allowed for serum/plasma to have immunodiagnostic tests performed. If no detection, he will submit to other types of specimen samples such as tissues, sputum, a vaginal swab or urine as requested by physician. Lastly, the physician is allowed to do an endoscopy, an X-ray, an MRI scan or a CT scan if other diagnostic procedures are not conclusive. There are huge samples to diagnose in specimen sample testing and less efficiency of the eggs detection result.

Generally, the larger the volume of the sample, the greater the chances for parasite detection following concentration; however, processing large volumes can be labor-intensive, time-consuming, costly, and can result in increased levels of contaminants which may interfere with subsequent detection methods. Whenever possible, faecal samples should be obtained directly from the animal to minimize the risk of cross-contamination, and prevent the introduction of parasites by insects. Thus, feces collected from the ground should be discarded if there is obvious evidence of insect activity. Ideally faecal samples should be processed within a few hours of collection or stored cold to prevent loss of moisture, overgrowth by fungi, and deterioration of antigen or DNA.

In this project, the automatic detection using techniques of image processing is proposed to detect the characteristics of parasite eggs. It has three stages that are image acquisition, processing stage, feature extraction stage, classification stage, and testing stage. In pre-processing stage, the digital image processing methods, which are noise reduction, contrast enhancement, thresholding, and morphological and logical processes. The process is continued with feature extraction and classification stage. The data will be tested using MATLAB software.

1.2 Project Objective

This project proposed a development of an automatic detection system to detect type of parasite in faecal sample using image processing technique. The techniques used in this project recognize the characteristics of eggs based on shape, smoothness and roundness.

1.3 Scopes Of Project

- i. Detection of eggs of two common human parasite worm, Roundworm (*Ascaris Lumbricoides*) and whipworm (*Trichuris Trichiura*)
- ii. Detection in microscopic image
- iii. Using image processing techniques
- iv. MATLAB software application

1.4 Problem Statement

- Diagnose of parasite is rely to human whereby microscope is used to detect parasite in a faecal sample. Due to huge sample of faecal to diagnose, technologies tend to make wrong result of detection. Otherwise, it is easier using microscopic image because it can be save inside computer's memory. Human fault is also a problem that cannot be prevented. Sometimes the doctor forgot about the characteristics of eggs of parasite and mistreated patient. Using software system, the source code is not easily change and the system will remembered the characteristics of egg of parasite to be determined. According to Hospital Universiti Sains Malaysia (HUSM), they received more than 100 sample of parasite per day. Generally, the larger the volume of the sample, the greater the chances for parasite detection following concentration; however, processing large volumes can be labor-intensive, time-consuming, costly, and can result in increased levels of contaminants which may interfere with subsequent detection methods.

Chapter 2

LITERATURE REVIEW

2.1 Literature review

– Dogantekin (2007) study proposed a robust technique based on invariant moments – adaptive network based fuzzy inference system (IM-ANFIS). In this technique, some digital image processing methods such as noise reduction, contrast enhancement, segmentation, and morphological process are used for feature extraction stage of IM-ANFIS approach used in this study.

In order to automate routine fecal examination for parasitic diseases, Yang (2001) paper propose in this study a computer processing algorithm using digital image processing techniques and an artificial neural network (ANN) classifier. The morphometric characteristics of eggs of human parasites in fecal specimens were extracted from microscopic images through digital image processing. An ANN then identified the parasite species based on those characteristics. He selected four morphometric features based on three morphological characteristics representing shape, shell smoothness, and size.

In Avci and Varol (2007) paper, it is proposed a new methodology based on invariant moments and multi-class support vector machine (MCSVM) for classification of human parasite eggs in microscopic images. The MCSVM is one of the most used classifiers but it has not used for classification of human parasite eggs to date. This method composes four stages. These are pre-processing stage, feature extraction stage, classification stage, and testing stage. In pre-processing stage, the digital image processing methods, which are noise reduction, contrast enhancement, thresholding, and morphological and logical processes. In feature extraction stage, the invariant moments of pre-processed parasite images are calculated. Finally, in classification stage, the multi-class support vector machine (MCSVM) classifier is used for classification of features extracted feature extraction stage. We used MATLAB software for estimating the success classification rate of proposed approach in this study. For this aim, proposed approach was tested by using test data. At end of test, 97.70% overall success rates were obtained.

Image segmentation remains one of the major challenges in image analysis, since image analysis tasks are often constrained by how well previous segmentation is accomplished. In particular, many existing image segmentation algorithms fail to provide satisfactory results when the boundaries of the desired objects are not clearly defined by the image intensity information. In medical applications, skilled operators are usually employed to extract the desired regions that may be anatomically separate but statistically indistinguishable. Such manual processing is subject to operator errors and biases, is extremely time consuming, and has poor reproducibility. Chen *et al.* (1998) propose a robust algorithm for the segmentation of three-dimensional (3-D) image data based on a novel combination of adaptive K-mean clustering and knowledge based morphological operations. The proposed adaptive K-mean clustering algorithm is capable of segmenting the regions of smoothly varying intensity distributions. Spatial constraints are incorporated in the clustering algorithm through the modeling of the regions by Gibbs random fields. Knowledge-based morphological operations are then applied to the segmented regions to identify the desired regions according to the a priori anatomical knowledge of the region-of-interest. This proposed technique has been successfully applied to a sequence of cardiac CT volumetric images to generate the volumes of

left ventricle chambers at 16 consecutive temporal frames. Their final segmentation results compare favorably with the results obtained using manual outlining. Extensions of this approach to other applications can be readily made when a priori knowledge of a given object is available.

Martin *et al.* (2010) present an example-based approach to synthesizing stipple illustrations for static 2D images that produces scale-dependent results appropriate for an intended spatial output size and resolution. They show how treating stippling as a grayscale process allows them to both produce on-screen output and to achieve stipple merging at medium tonal ranges. At the same time they can also produce images with high spatial and low color resolution for print reproduction. In addition, they discuss how to incorporate high-level illustration considerations into the stippling process based on discussions with and observations of a stipple artist. Also, certain features such as edges can be extracted and used to control the placement of dots to improve the result. The implementation of the technique is based on a fast method for distributing dots using halftoning and can be used to create stipple images interactively. They describe both a GPU implementation of the basic algorithm that creates stipple images in real-time for large images and an extended CPU method that allows a finer control of the output at interactive rates.

Advances in visualization technology and specialized graphic workstations allow clinicians to virtually interact with anatomical structures contained within sampled medical-image datasets. A hindrance to the effective use of this technology is the difficult problem of image segmentation. In Shareef *et al.*(1999) paper, they utilize a recently proposed oscillator network called the locally excitatory globally inhibitory oscillator network (LEGION) whose ability to achieve fast synchrony with local excitation and desynchrony with global inhibition makes it an effective computational framework for grouping similar features and segregating dissimilar ones in an image. They extract an algorithm from LEGION dynamics and propose an adaptive scheme for grouping. They show results of the algorithm to two-dimensional (2-D) and three-dimensional (3-D) (volume) computerized topography

(CT) and magnetic resonance imaging (MRI) medical-image datasets. In addition, they compare their algorithm with other algorithms for medical-image segmentation, as well as with manual segmentation. LEGION's computational and architectural properties make it a promising approach for real-time medical-image segmentation.

Multiscale image analysis has been used successfully in a number of applications to classify image features according to their relative scales. As a consequence, much has been learned about the scale-space behavior of intensity extrema, edges, intensity ridges, and grey-level blobs. In Gauch (1999) paper, they investigate the multiscale behavior of gradient watershed regions. These regions are defined in terms of the gradient properties of the gradient magnitude of the original image. Boundaries of gradient watershed regions correspond to the edges of objects in an image. Multiscale analysis of intensity minima in the gradient magnitude image provides a mechanism for imposing a scale-based hierarchy on the watersheds associated with these minima. This hierarchy can be used to label watershed boundaries according to their scale. This provides valuable insight into the multiscale properties of edges in an image without following these curves through scale-space. In addition, the gradient watershed region hierarchy can be used for automatic or interactive image segmentation. By selecting subtrees of the region hierarchy, visually sensible objects in an image can be easily constructed.

Chapter 3

METHODOLOGY

3.1 Introduction

This chapter explains all of methodology for this project. It describes on how these project is organized which is the flow of step in order to complete the project.

3.2 System flow

The system flow of image processing technique is shown in Figure 3.1.

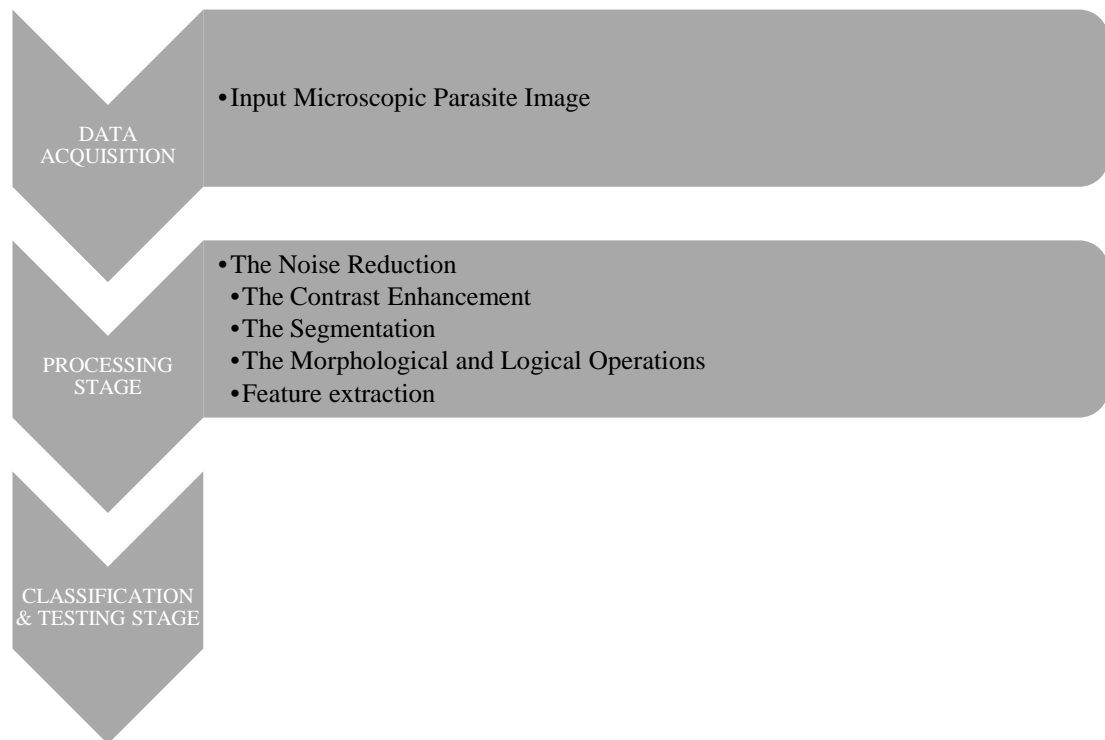


Figure 3.1: Processing stage

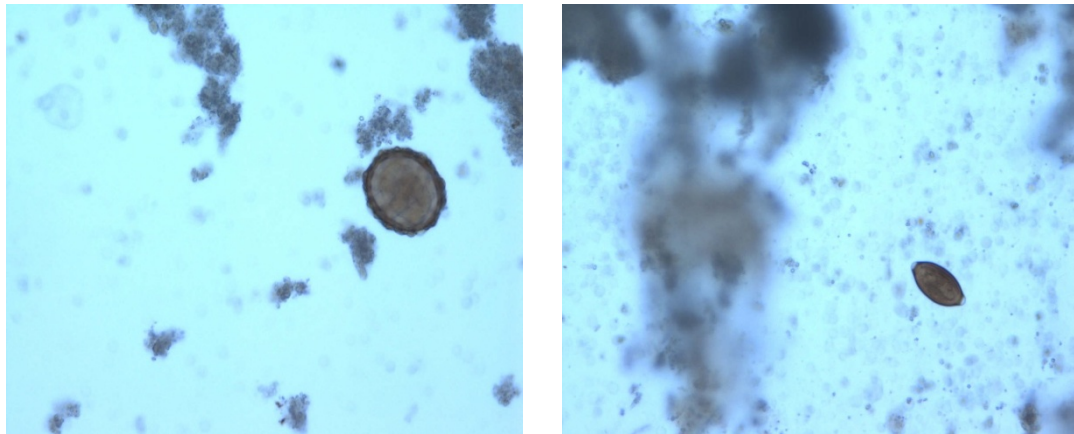
3.2.1 Eggs of Parasite Data Information

The image data of two types of parasites are collected by using microscope available at HUSM located at Kubang Kerian, Kelantan.. The sample of the parasites which comes from the faecal is provided by the doctor at HUSM.



Figure 3.2: HUSM at Kubang Kerian

The microscope used has three different resolutions which is high resolution value that reduced noise in image acquired. Figure 3.2 shows the two images of two types of parasite worms. We can see the difference between both eggs.



(a)

(b)

Figure 3.3: Microscopic input image of a) Roundworm b) Whipworm

The microscope used has three different resolutions (10 nm, 20 nm and 40 nm) which is high resolution value that reduced noise in image acquired. Number of images of Roundworm is 64 images for 10 nm, 16 images for 20 nm, 63 images for 40 nm. Number of images of Whipworm is 20 images for 10 nm, 20 nm and 40 nm. All image acquired in .JPG format files. Total sizes of images of Roundworm are 12.6 MB. Total sizes of images of Whipworm are 5.55 MB. JPEG is a commonly used method of lossy compression for digital photography (image). The JPEG compression algorithm is at its best on photographs and paintings of realistic scenes with smooth variations of tone and color. The JPEG are compressed and take up much less room than a TIFF, BMP, or RAW. Most items that allow saving under a JPG also allow how much it is compressed.

3.2.2 Processing image

In first step, the processing is used for improvise the RGB image that have been captured due to some disturbance and distortion that occurred while collecting the data information. Collecting data by capturing from camera will lead to some noise. From previous step, the data information will enhance and the noise has been removed. The image is been read and the total bytes of the image is 112 bytes. The *h* or *vision* at *hcsc* functioned to create color space converter with same property values. The *hidtypeconv* converted and scaled input image to specified output data type which is 'single'.

```
hcsc = vision.ColorSpaceConverter('Conversion', 'RGB to intensity');
hidtypeconv = vision.ImageDataTypeConverter('OutputDataType','single');
```

Secondly in processing stage, we make an edge detection to outline all the objects in the image. The Sobel edge detector is used as the default edge detection. The *h* or *vision* at *hidtypeconv* create edge detector object with same value. The *hcsc* is a morphological dilate class that dilate on an intensity class. It fused fine discontinuities on images. The step has been performed morphological dilate on input.

```
hedge = vision.EdgeDetector;
hcsc = vision.ColorSpaceConverter('Conversion', 'RGB to intensity');
hidtypeconv = vision.ImageDataTypeConverter('OutputDataType','single');
% read image and perform morphological dilate
=step(hcsc,imread('C:\Users\Documents\psm\Roundworm,Ascaris
lumbricoides\ALO ClearImages\10\2.jpg'));
step(hidtypeconv, img);
edges = step(hedge, img1);
```

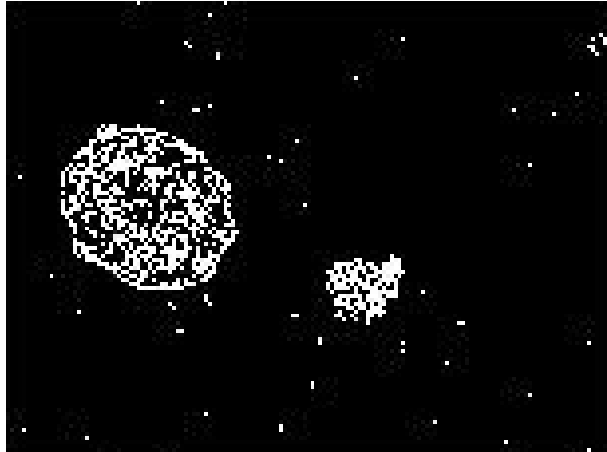


Figure 3.4: The appeared edges image

Then, we do the dilation image to make the edge that had been outlined clearer. The *imdilate* showed lines of high contrast using of the structuring element of length 3 and the degree of 90 and 0.

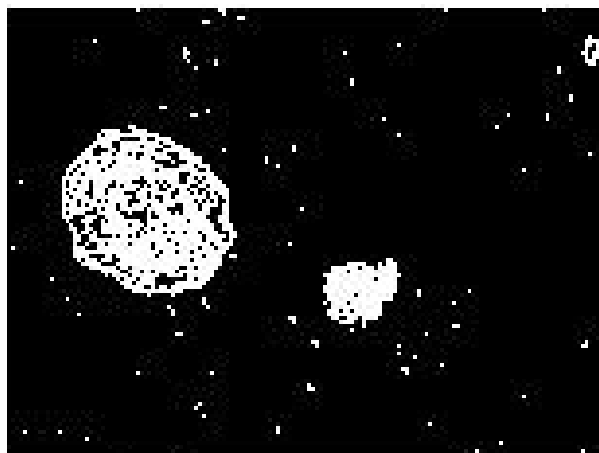


Figure 3.5: The dilated image

```
se90 = strel('line', 3, 90);  
se0 = strel('line', 3, 0);  
% shows lines of high contrast  
bwdil = imdilate(edges, [se90 se0]);
```

The filling is followed after that to fill the holes inside image.

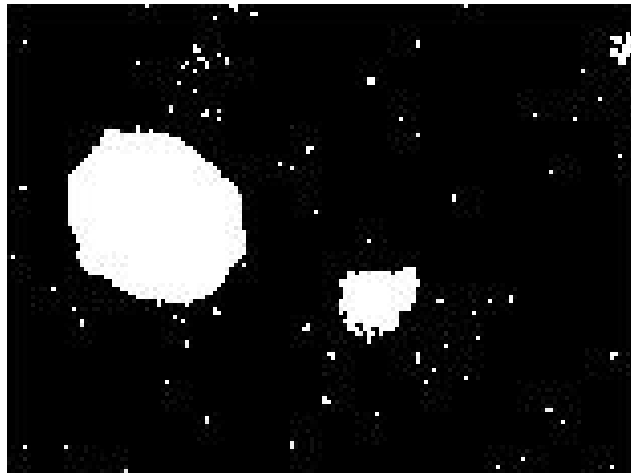


Figure 3.6: The filling image

```
bwdfill = imfill(bwdil, 'holes');
```

After that, we cleared the image at the border of image to make the detection easier. The *imclearborder* suppressed structures that are lighter than their surroundings and that are connected to the image border. The 4 size of mask have been chosen.

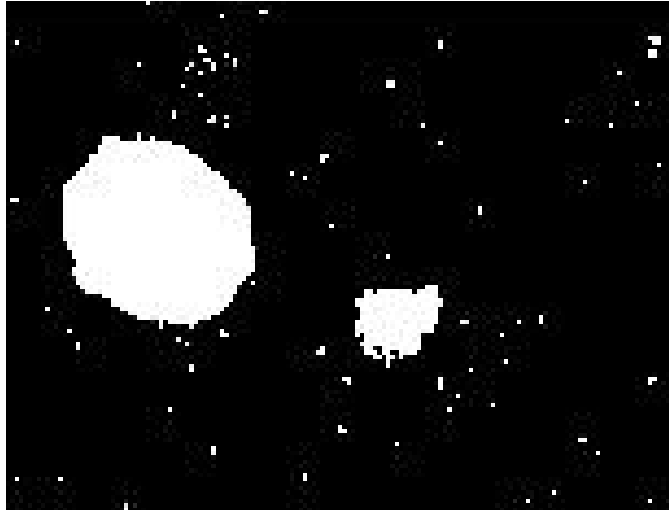


Figure 3.7: The cleared border image

```
bwnobord = imclearborder(bwdfill, 4);
```

The erosion then deleted image that having a radius less than 8 by 8 pixels by opening it with the disk-shaped structuring element. The N that is 8 is approximated by a sequence of N periodic-line structuring elements. Morphological operations run much faster when the structuring element uses approximations ($N > 0$) than when it does not ($N = 0$). However, structuring elements that do not use approximations ($N = 0$) are not suitable for computing granulometries.

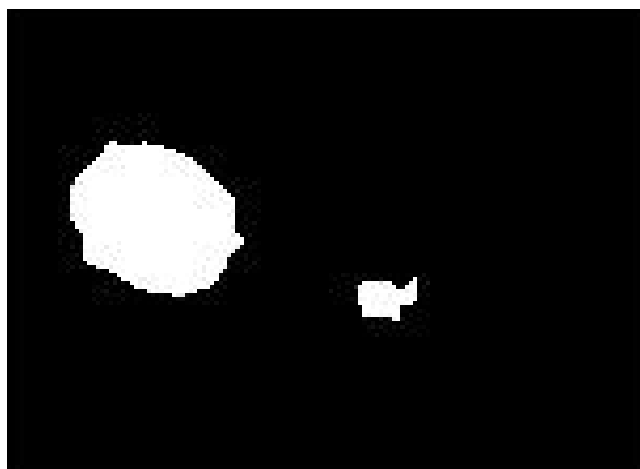


Figure 3.8: The eroded image

```

seD = strel('disk',8,8);
bwfinal2 = imerode(bwnobord,seD);
bwfinal = imerode(bwfinal2,seD);

```

Thresholding technique is suitable for this process. This technique allow only the setting shape which is round for remain in picture. The other shape out of setting will be removed. *Bwboundaries* traced the exterior boundaries of objects, as well as boundaries of holes inside these objects, in the binary image BW. It searched only for object (parent and child) boundaries. This can provide better performance. *Label2rgb* assigned colormap colors to regions in the label matrix. The code read in and threshold an intensity image. It displayed the labeled objects using the jet colormap, on a gray background, with region boundaries outlined in white. The roundness is estimated each object's area and perimeter. These results are used to form a simple metric indicating the roundness of an object:

$$metric = 4*pi*area/perimeter^2$$

This metric is equal to one only for a circle and it is less than one for any other shape. The discrimination process can be controlled by setting an appropriate threshold. In this example a threshold of 0.94 is used so that only the pills will be classified as round.

Use *regionprops* to obtain estimates of the area for all of the objects. Notice that the label matrix returned by *bwboundaries* can be reused by *regionprops*.



Figure 3.9: The final result

```

[ B,L] = bwboundaries(bwfinal,'noholes');
% Display the label matrix and draw each boundary
imshow(label2rgb(L, @jet, [.5 .5 .5]))
hold on
for k = 1:length(B)
    boundary = B{k};
    plot(boundary(:,2), boundary(:,1), 'w', 'LineWidth', 2)
End
stats = regionprops(L,'Area','Centroid');
threshold = 0.94;
% loop over the boundaries
for k = 1:length(B)
% obtain (X,Y) boundary coordinates corresponding to label 'k'
    boundary = B{k};
    % compute a simple estimate of the object's perimeter
    delta_sq = diff(boundary).^2;
    perimeter = sum(sqrt(sum(delta_sq,2)));
    % obtain the area calculation corresponding to label 'k'
    area = stats(k).Area;
    % compute the roundness metric
    metric = 4*pi*area/perimeter^2;

```

```
% display the results  
metric_string = sprintf('%2.2f',metric);  
% mark objects above the threshold with a black circle  
if metric > threshold  
centroid = stats(k).Centroid;  
plot(centroid(1),centroid(2),'ko');  
end  
text(boundary(1,2)-35,boundary(1,1)+13,metric_string,'Color','y',  
'FontSize',14,'FontWeight','bold');  
end
```

3.2.3 Making Decision

The characteristic of roundness of the egg will be detected by the system invented. The program will calculate the roundness metric of the subject detected in the final image. The equation used is $4\pi\text{area}/\text{perimeter}^2$. The value that is near to 1 is approximately round.

Chapter 4

RESULTS AND DISCUSSIONS

4.1 Results

4.1.1 Roundworm, Ascaris Lumbricoides

Figure 4.1 shows the desired eggs appear with its size at 0.85 for Roundworm, *Ascaris Lumbricoides*. The figure is a microscopic image with 10 nm resolutions. Other subjects are also been detected.

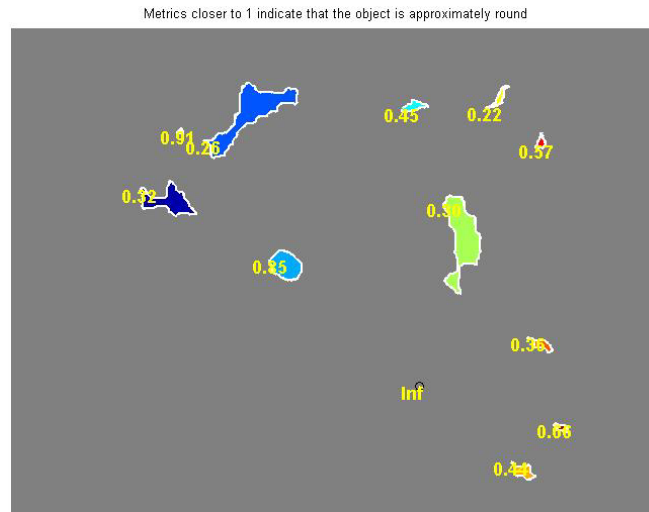


Figure 4.1: Detected Roundworm eggs with 10 nm resolutions

Figure 4.2 shows step by step of image processing technique for 10nm resolutions image. The step starts with edge detection, followed by dilated gradient mask, binary image with filled holes, cleared border image, segmented image and lastly metrics closer to 1 indicate that the object is approximately round.

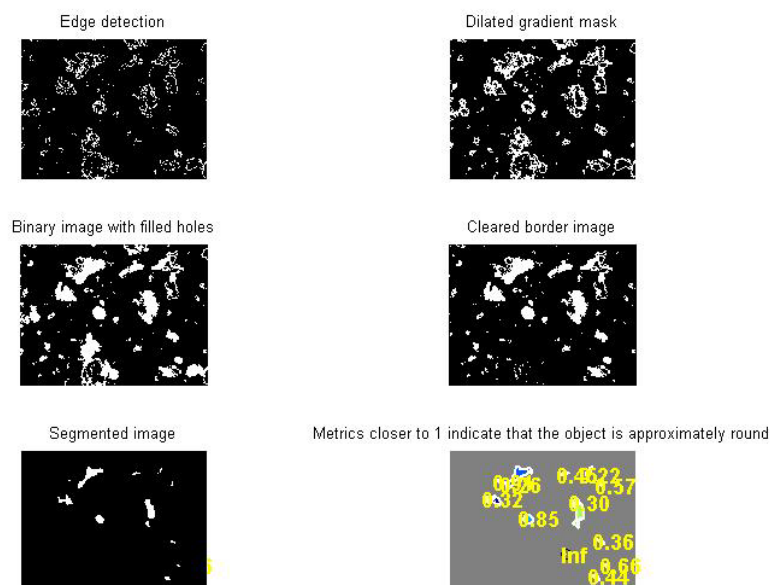
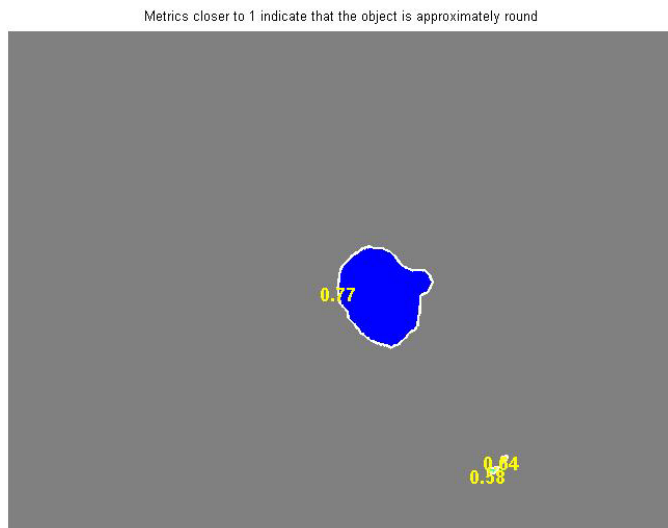


Figure 4.2: Step by step to detect the Roundworm egg with 10 nm resolutions

Figure 4.3 shows smoother detection of Roundworm parasite using 20nm resolutions than using 10nm resolutions.



Figure

4.3: Detected Roundworm eggs with 20 nm resolutions

The procedural process to get Roundworm, *Ascaris Lumbricoides* detected image using 20nm resolutions is shown in Figure 4.4.

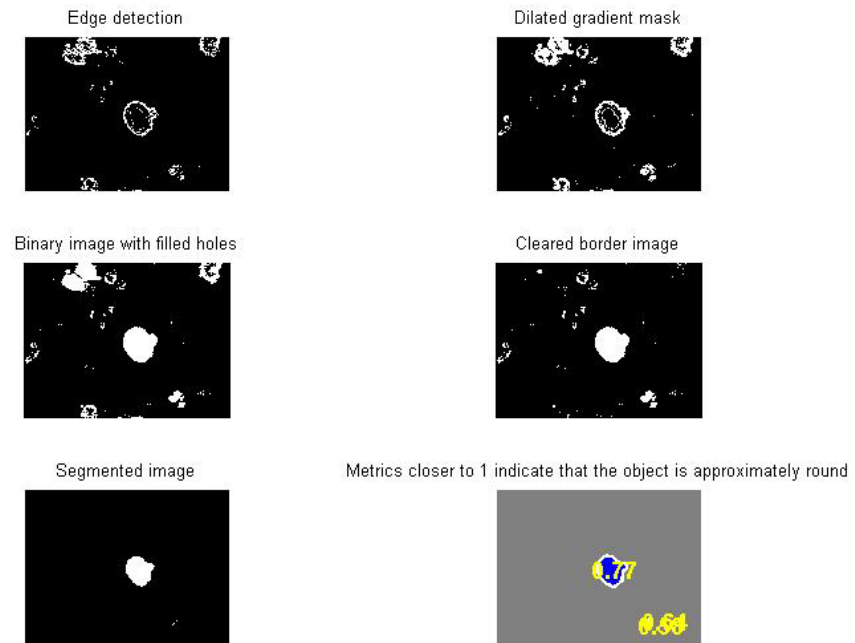


Figure 4.4: Step by step to detect the Roundworm egg with 20 nm resolutions

Figure 4.5 shows Roundworm, *Ascaris Lumbricoides* egg with another subject detected. Even though this system could not detect only Roundworm egg, but it is better than when using 10nm and 20nm resolutions.

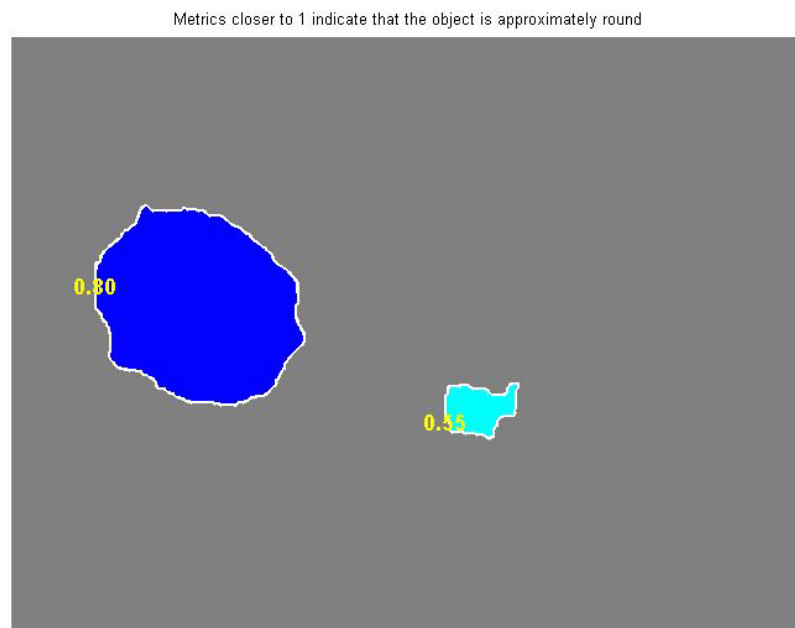


Figure 4.5: Detected Roundworm eggs with 40 nm resolutions

Figure 4.6 shows step by step image to get final image which detected the Roundworm, *Ascaris Lumbricoides* using 40 nm resolutions.

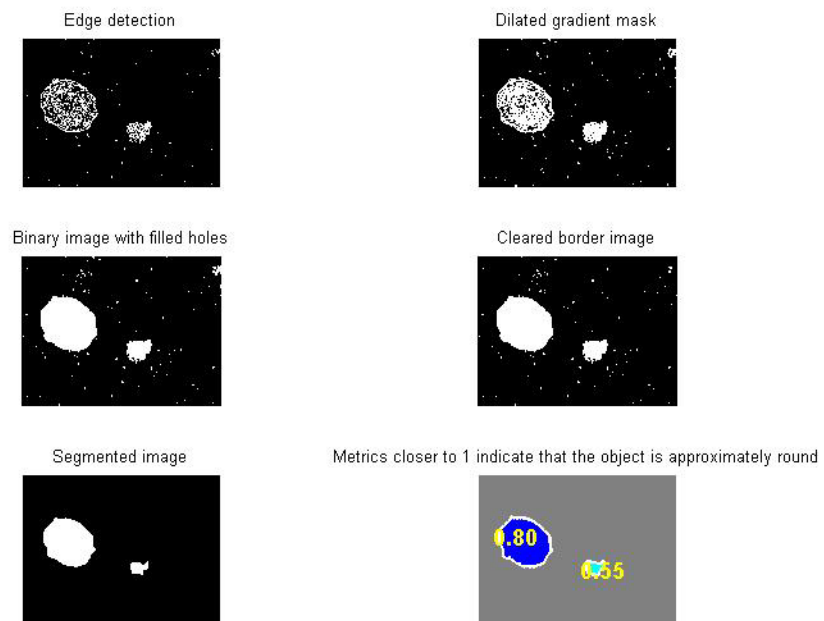


Figure 4.6: Step by step to detect the Roundworm egg with 40 nm resolutions

4.1.2 Whipworm, *Trichuris Trichiura*

Figure 4.7 shows the Whipworm, *Trichuris Trichiura* which had been detected alone using 10 nm resolutions. This approved my system can automatically detected the egg of the parasite.

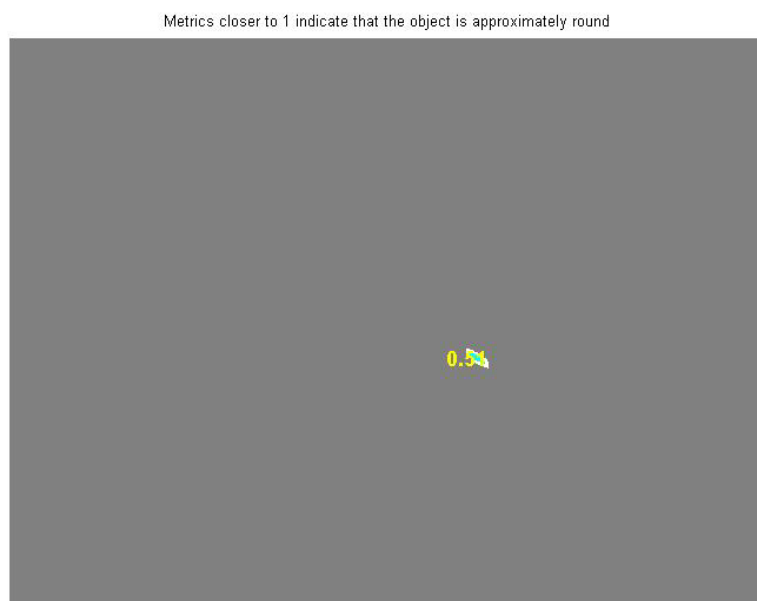


Figure 4.7: Detected Whipworm eggs with 10 nm resolutions

Figure 4.8 shows step by step process to get the Whipworm, *Trichuris Trichiura* detected using 10 nm resolutions.

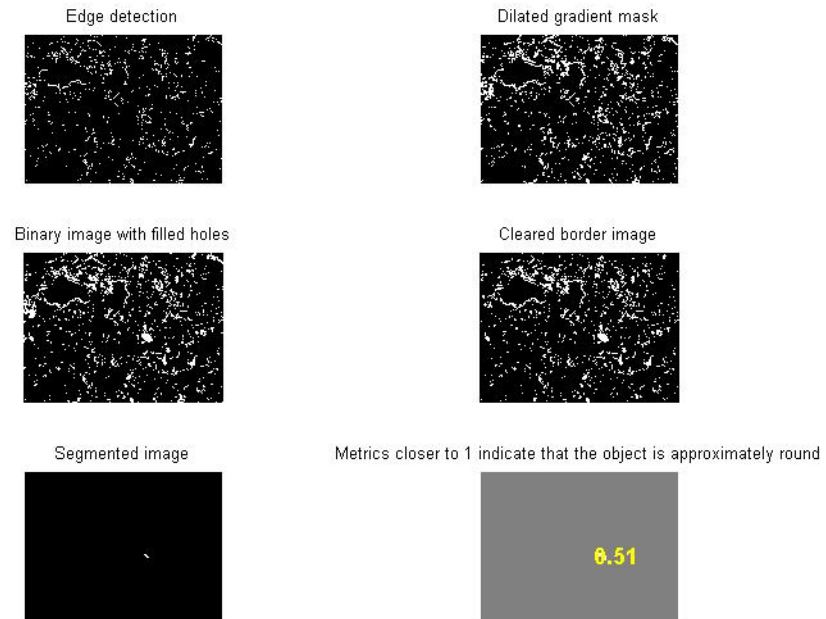


Figure 4.8: Step by step to detect the Whipworm egg with 10 nm resolutions

Figure 4.9 shows the roundness of the Whipworm egg made the image of the egg which using 20 nm resolutions appeared as good as detecting the Whipworm egg using image of 10 nm resolutions.



Figure 4.9: Detected Whipworm eggs with 20 nm resolutions

The procedural process to get Whipworm, *Trichuris Trichiura* detected which using 20nm resolutions image is shown in Figure 4.10.

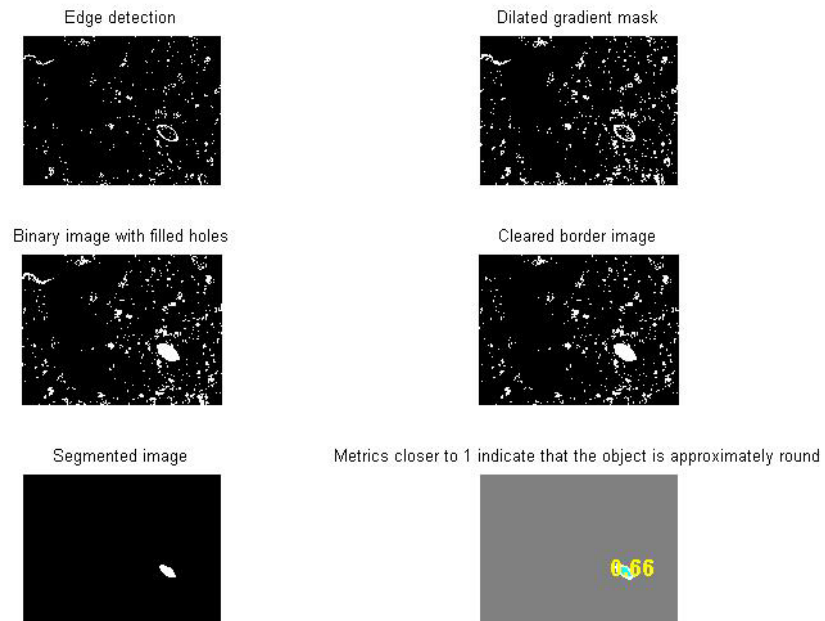


Figure 4.10: Step by step to detect the Whipworm egg with 20 nm resolutions

Figure 4.11 shows the image of the egg of Whipworm, *Trichuris Trichiura* with two other subjects detected using 40 nm resolutions.



Figure 4.11: Detected Whipworm eggs with 40 nm resolutions

Figure 4.6 shows step by step image to get final image which detected the Whipworm, *Trichuris Trichiura* using 40 nm resolutions.

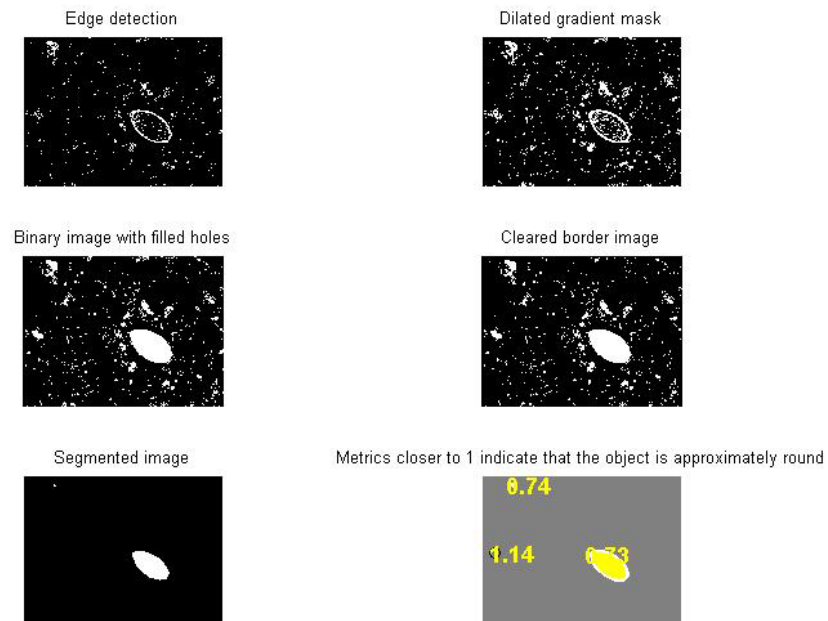


Figure 4.12: Step by step to detect the Whipworm egg with 40 nm resolutions

4.1.3 Size of roundness of detected eggs

Table 4.1 shows the difference result of size between image of the egg of Roundworm, *Ascaris Lumbricoides* and Whipworm, *Trichuris Trichiura* using 10 nm resolutions. It shows that the size for Roundworm, *Ascaris Lumbricoides* egg is from 0.8 to 0.88. While for Whipworm, *Trichuris Trichiura* egg, the size is from 0.43 to 0.51. The Roundworm egg is bigger than the Whipworm egg.

Table 4.2 shows the difference result of size between image of the egg of Roundworm, *Ascaris Lumbricoides* and Whipworm, *Trichuris Trichiura* using 20 nm resolutions. It shows that the size for Roundworm, *Ascaris Lumbricoides* egg is from

0.69 to 0.83. While for Whipworm, *Trichuris Trichiura* egg, the size is from 0.41 to 0.66.

Table 4.3 shows the difference result of size between image of the egg of Roundworm, *Ascaris Lumbricoides* and Whipworm, *Trichuris Trichiura* using 40 nm resolutions. It shows that the size for Roundworm, *Ascaris Lumbricoides* egg is from 0.58 to 0.8. While for Whipworm, *Trichuris Trichiura* egg, the size is from 0.39 to 0.73. The Roundworm egg is bigger than the Whipworm egg.

The input images that had been recorded in Table 4.1, Table 4.2 and Table 4.3 can be review in Appendix A.

Table 4.1: The size of eggs image with 10 nm resolutions

Resolution	10nm				
Picture No	1	2	3	4	5
Roundworm	0.85	0.88	0.8	0.83	0.87
Whipworm	0.51	0.43	0.51	0.47	0.47

Table 4.2: The size of eggs image with 10 nm resolutions

Resolution	10nm				
Picture No	6	7	8	9	10
Roundworm	0.86	0.41	0.88	0.85	0.82
Whipworm	0.60	0.57	0.58	0.35	0.46

Table 4.3: The size of eggs image with 20 nm resolutions

Resolution	20nm				
Picture No	1	2	3	4	5
Roundworm	0.82	NULL	0.82	0.83	0.87
Whipworm	0.64	0.64	0.66	0.59	NULL

Table 4.4: The size of eggs image with 20 nm resolutions

Resolution	20nm				
Picture No	6	7	8	9	10
Roundworm	0.77	NULL	0.69	0.83	0.73
Whipworm	0.66	0.64	0.55	0.41	0.64

Table 4.5: The size of eggs image with 40 nm resolutions

Resolution	40nm				
Picture No	1	2	3	4	5
Roundworm	0.8	NULL	0.83	0.58	NULL
Whipworm	0.73	0.67	0.49	0.39	0.69

Table 4.6: The size of eggs image with 40 nm resolutions

Resolution	40nm				
Picture No	6	7	8	9	10
Roundworm	0.8	NULL	0.83	0.58	NULL
Whipworm	0.68	0.69	0.69	0.62	NULL

4.2 Discussion

The roundness of both types of parasite eggs had been detected but there are other noise also detected. The research will continue whether to set the threshold value for each eggs or forwarding the enhancement image to the doctor for the type of parasite to be determined. The filter to remove the noise also can be proposed. The egg of Roundworm is bigger in roundness size than the egg of Whipworm.

The higher spatial resolution of a digital image, the more accurate the image which more details on the image will be captured, but the disadvantage of high resolution images are the large number of memory required to keep all the data. However, it also depends on the desired function of the system. For this research, the requirement for high resolution is none because all resolution shows same improvement of image.

Three sample out of 30 samples of all result image gave automatic detection. Overall performance for this system is 73%. For the 10 nm resolutions 100% samples is detected while for 20nm and 40nm resolutions, the performance are 70% and 50% respectively.

Chapter 5

CONCLUSION

5.1 Conclusion

The development of an automatic detection system is achieved. The system detects the types of parasite which are Roundworm, Ascaris Lumbricoides and Whipworm, Trichuris Trichiura which are in microscopic image. The technique used for detection is image processing. The eggs are recognized according to its shape, smoothness and roundness. The application of MATLAB software to simulate image processing technique is successfully done. This is important for the medical world as this method is effortless, save time and cost.

5.2 Recommendation

- This research can be improved by using integration with microscope to make automatic detection of egg of human common parasites. The embedded system FPGA can be used to integrate the system with the microscope.



Figure 5.1: Microscope with system integration



Figure 5.2: Embedded system FPGA

REFERENCE

- [1] Avci, D., Varol, A., (2007). *An expert diagnosis system for classification of human parasite eggs based on multi-class SVM*. Expert Systems with Applications. Available at: <http://www.sciencedirect.com.ezproxy.ump.edu.my/>
- [2] Dogantekin, E., (2007). *A robust technique based on invariant moments – ANFIS for recognition of human parasite eggs in microscopic images*. Expert Systems with Applications. Available at: <http://www.sciencedirect.com.ezproxy.ump.edu.my/>
- [3] Chen, C. W., (1998). *Image Segmentation via Adaptive K-Mean Clustering and Knowledge-Based Morphological Operations with Biomedical Applications*. IEEE Transactions on Image Processing. Available at: <http://ieeexplore.ieee.org.ezproxy.ump.edu.my/Xplore/guesthome.jsp>
- [4] Yang, Y. S., (2001). *Automatic Identification of Human Helminth Eggs on Microscopic Fecal Specimens Using Digital Image Processing and an Artificial Neural Network*. IEEE Transactions on Biomedical Engineering. Available at: <http://ieeexplore.ieee.org.ezproxy.ump.edu.my/Xplore/guesthome.jsp>
- [5] Jaseema Yasmin, J.H., (2011). *Robust segmentation algorithm using LOG edge detector for effective border detection of noisy skin lesions*. Computer, Communication and E. Available at: <http://www.sciencedirect.com.ezproxy.ump.edu.my/>
- [6] Martin, D., (2010). *Scale-dependent and example-based grayscale stippling*. Computers & Graphics. Available at: <http://www.sciencedirect.com.ezproxy.ump.edu.my/>

[7] Ortiz-Garcia, E.G., (2007). *Automated generation and visualization of picture-logic puzzles*. Computers & Graphics.

Available at: <http://www.sciencedirect.com.ezproxy.ump.edu.my/>

[8] Czerwinski, R.N., (1998). *Line and Boundary Detection in Speckle Images*. IEEE Transactions on Image Processing.

Available at: <http://ieeexplore.ieee.org.ezproxy.ump.edu.my/Xplore/guesthome.jsp>

[9] Gauch, J.M., (1999). *Image Segmentation and Analysis via Multiscale Gradient Watershed Hierarchies*. IEEE Transactions on Image Processing.

Available at: <http://ieeexplore.ieee.org.ezproxy.ump.edu.my/Xplore/guesthome.jsp>

[10] Krumhardt, Barbera, PhD. Human Parasites. 08 October 2008

[11] 196 D.S. Zarlenga, J.M. Trout / Veterinary Parasitology 126 (2004) 195–217

[12] Camps-Valls, G., Tuia, D., Gómez-Chova, L., Jiménez, S., Malo, J., (2012). *Remote sensing image processing*. Synthesis Lectures on Image, Video, and Multimedia Processing.

Available at: <http://www.scopus.com/home.url>

[13] Elmasry, G., Cubero, S. Moltó, E., Blasco, J., (2012). *In-line sorting of irregular potatoes by using automated computer-based machine vision system*. Journal of Food Engineering.

Available at: <http://www.scopus.com/home.url>

[14] Vijayakumar, J., Arumugam, S., (2012). *Study of betelvine plants diseases and methods of disease identification using digital image processing*. European Journal of Scientific Research.

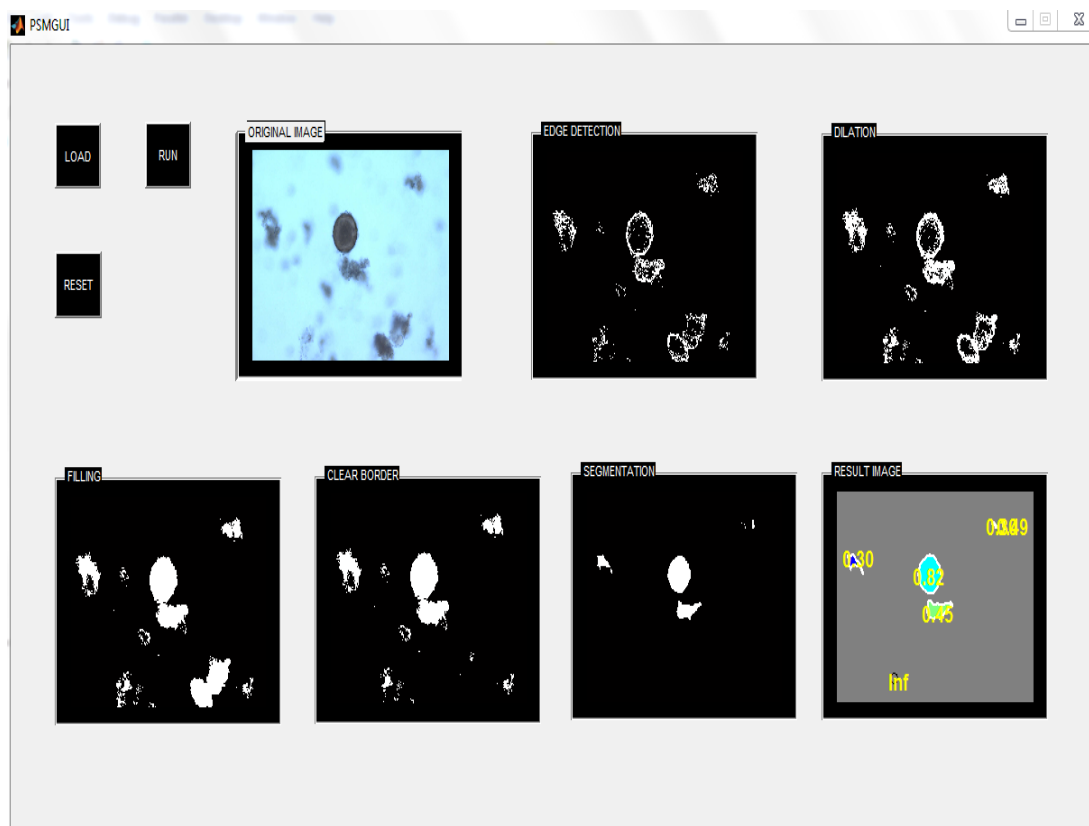
Available at: <http://www.scopus.com/home.url>

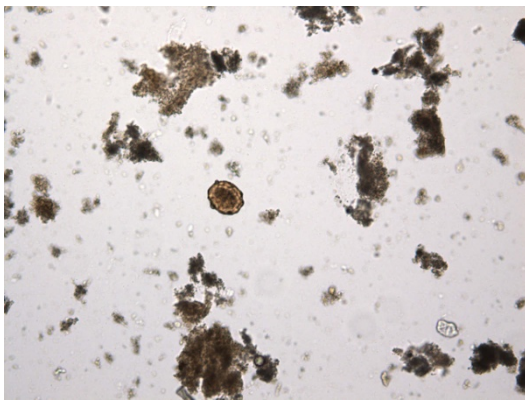
[15] Datta, S., Chakraborty, M., *Patellar fracture analysis using segmentation and global thresholding techniques*. Communications in Computer and Information Science.

Available at: <http://www.scopus.com/home.url>

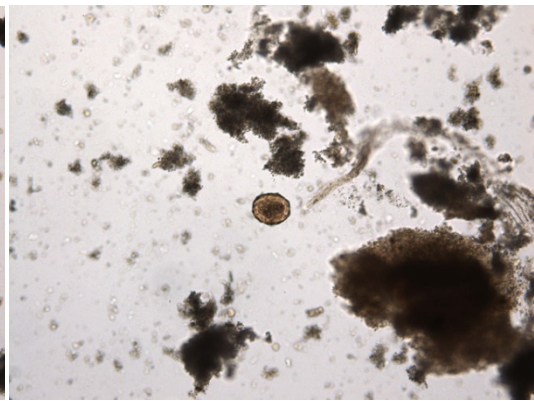
APPENDIX A

GUI Builder

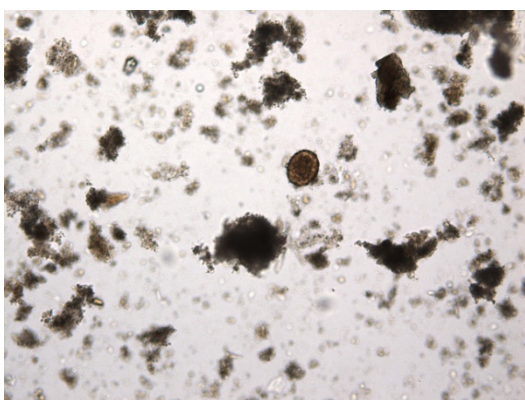


APPENDIX B**Input Images****Input images of Roundworm, *Ascaris Lumbricoides*****Images using 10 nm resolutions**

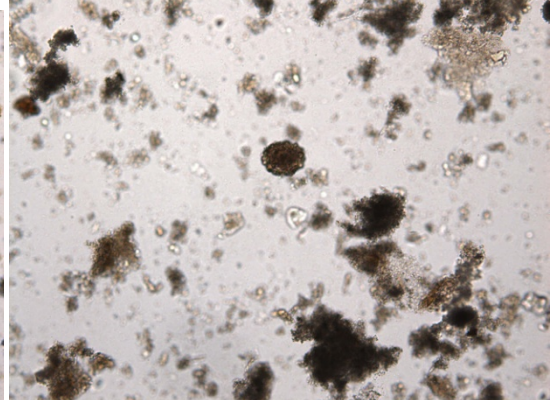
(1)



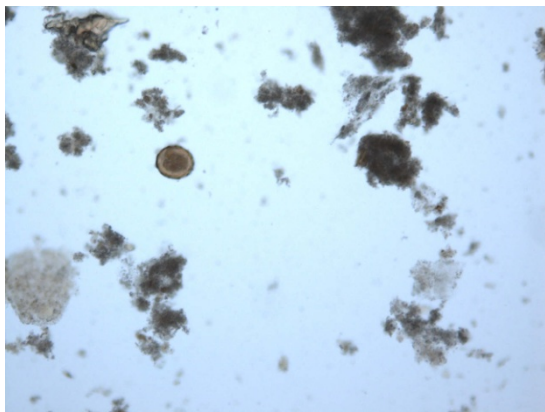
(2)



(3)

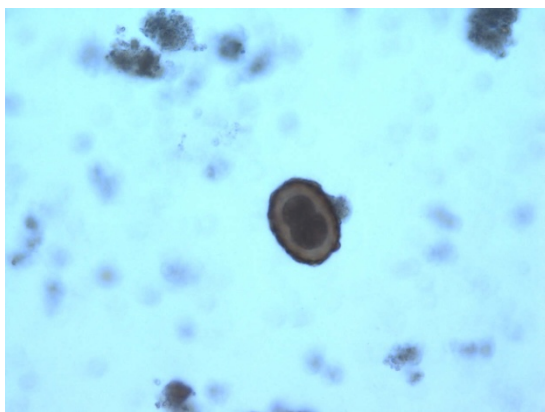


(4)

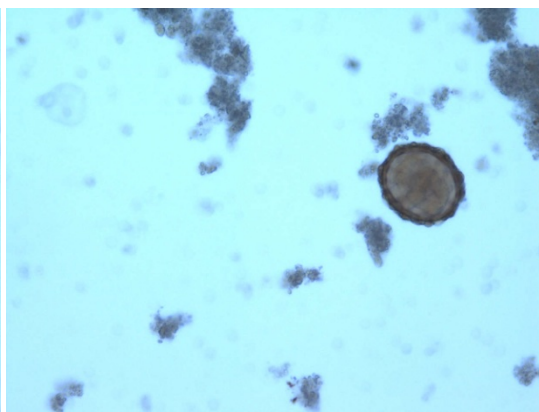


(5)

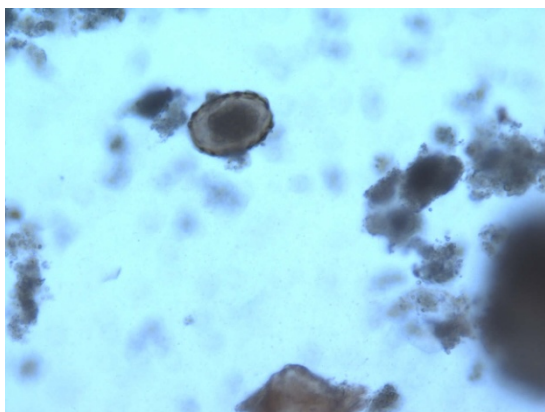
Images using 20 nm resolutions



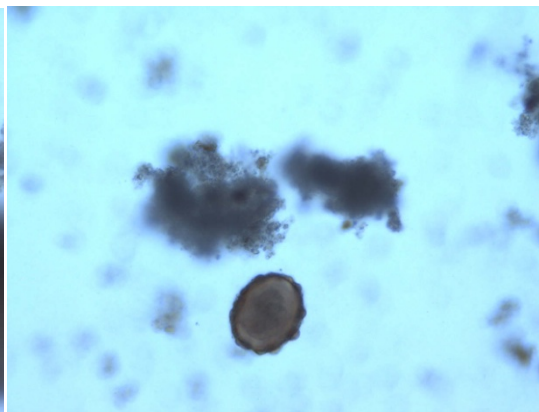
(1)



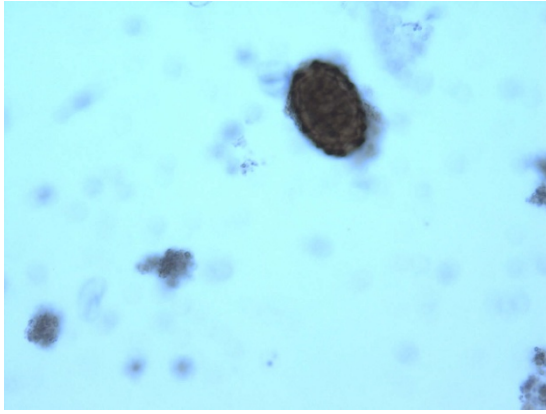
(2)



(3)

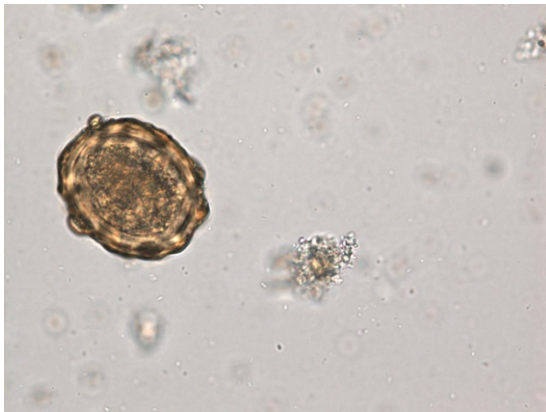


(4)

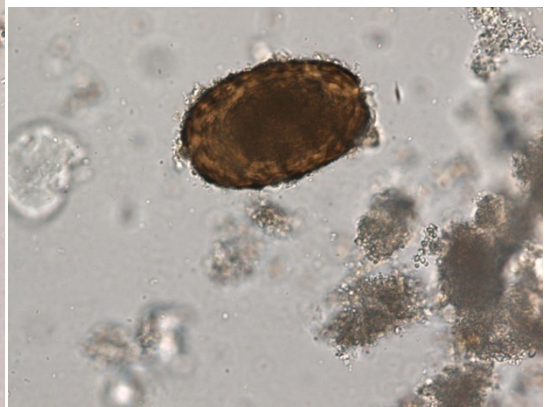


(5)

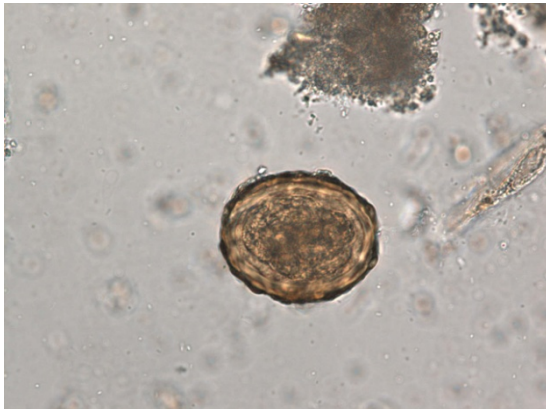
Images using 40 nm resolutions



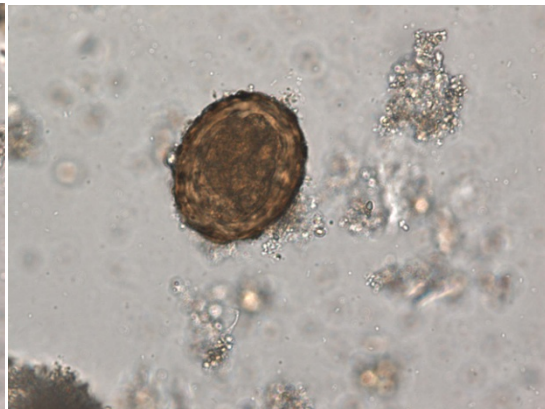
(1)



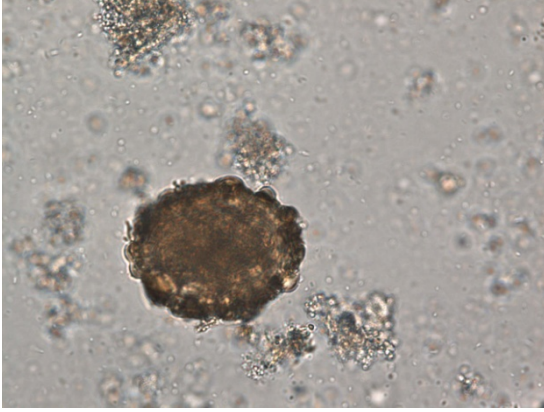
(2)



(3)



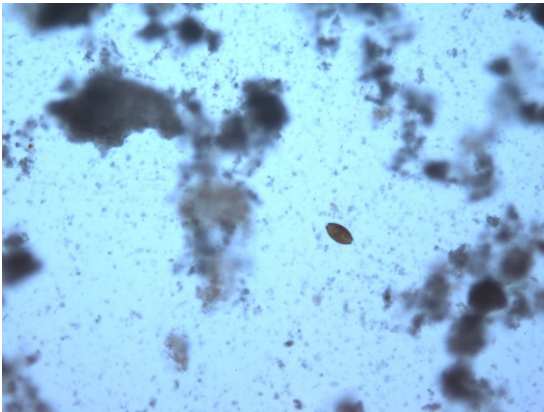
(4)



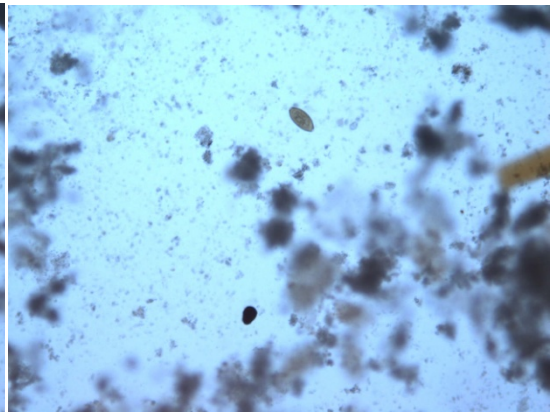
(5)

Input images of Whipworm, Trichuris Trichuria

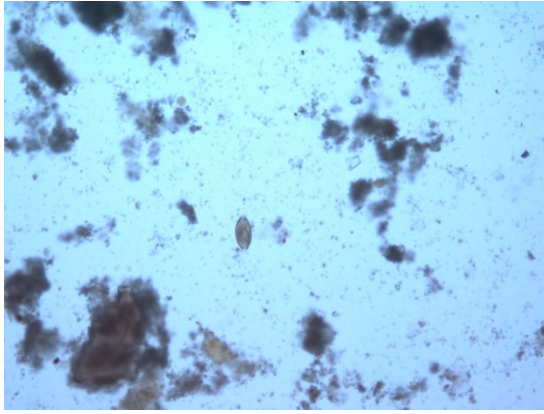
Images using 10 nm resolutions



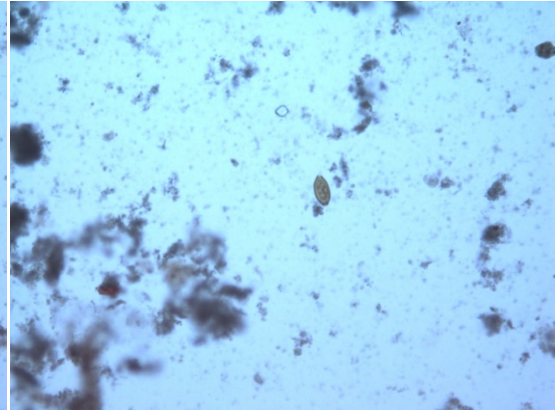
(1)



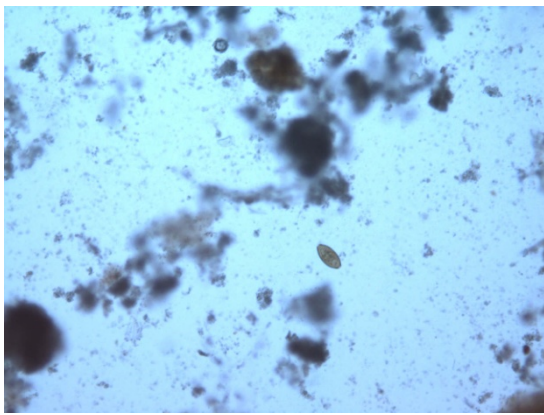
(2)



(3)

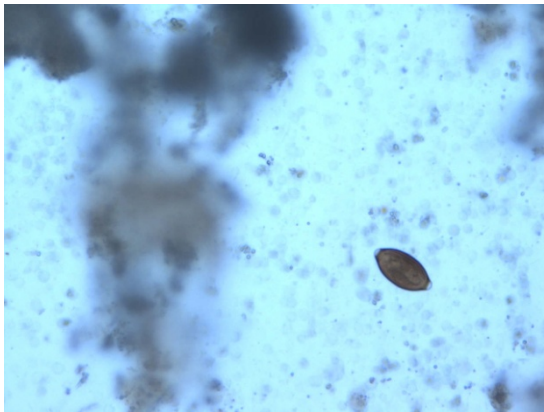


(4)

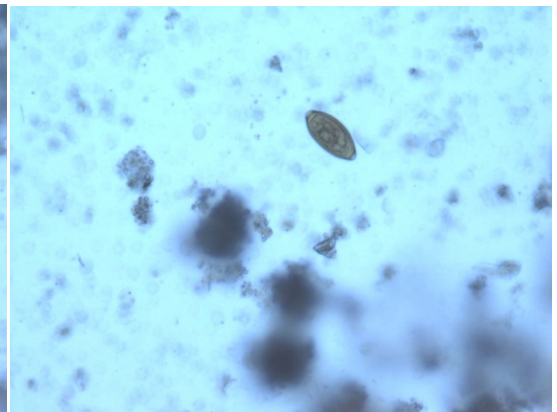


(5)

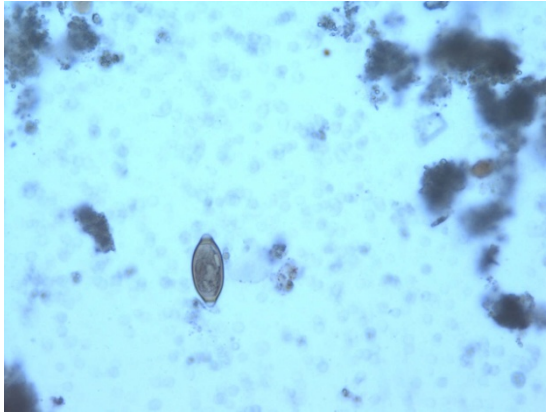
Images using 20 nm resolutions



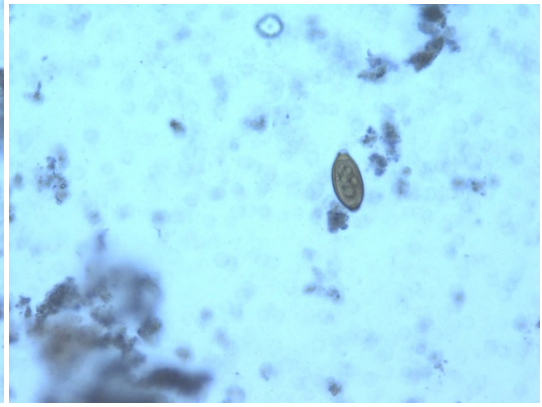
(1)



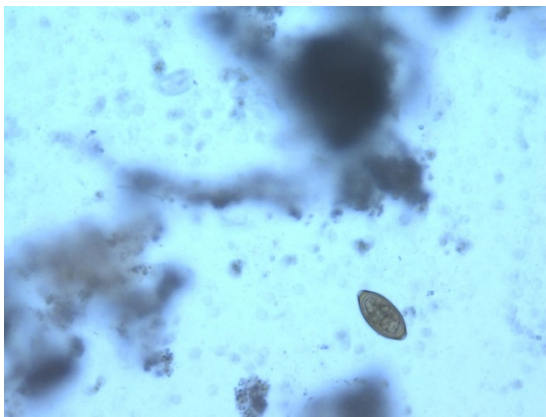
(2)



(3)

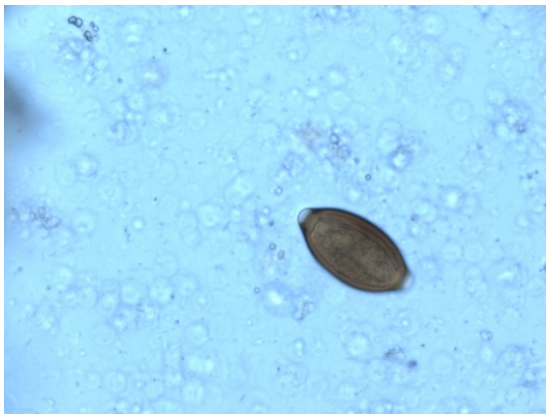


(4)

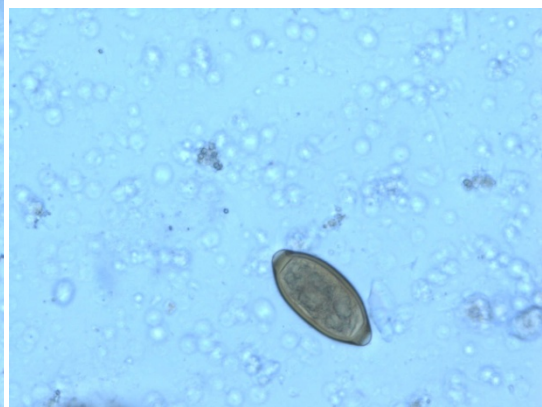


(5)

Images using 40 nm resolutions



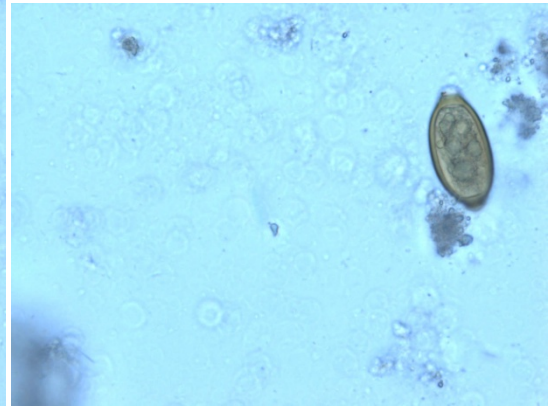
(1)



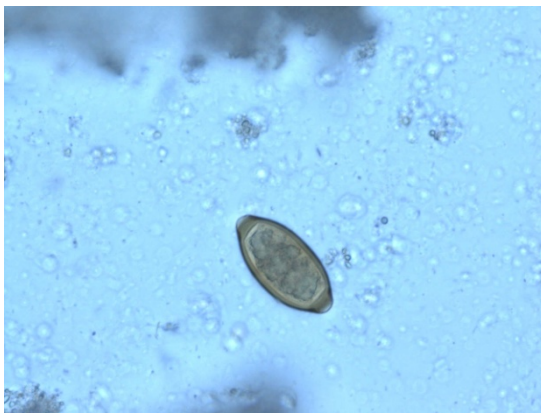
(2)



(3)



(4)



(5)